Cu(I) Camphor Coordination Polymers: Synthesis and Study of the Catalytic Activity for Cyclization of 4-Pentyn-1-oic Acid

Tiago A. Fernandes,[1] Adelino M. Galvão,[1] Ana M. Botelho do Rego,[2] M. Fernanda N. N. Carvalho[1]

[1]Centro de Química Estrutural, Instituto Superior Técnico, Universidade de Lisboa, Av. Rovisco Pais, 1049-001 Lisboa, Portugal
[2]Centro de Química-Física Molecular (CQFM) and Institute of Nanoscience and Nanotechnology (IN), Instituto Superior Técnico, Universidade de Lisboa, Av. Rovisco Pais, 1049-001 Lisboa, Portugal
Correspondence to: M. F. N. N. Carvalho (E-mail: fcarvalho@ist.utl.pt)

Received 6 June 2014; accepted 1 September 2014; published online 19 September 2014
DOI: 10.1002/pola.27393

ABSTRACT: The number of CuCl units *per* camphor ligand in $[\{CuCl\}_2L]_n$ was extended to three or four in $[\{CuCl\}_3L]_n$ (**2**) or $[\{CuCl\}_4L]_n$ (**1**). The Hartree-Fock *ab initio* calculations support the polymeric structure of **1** and **2** that catalyze the cyclization of 4-pentyn-1-oic acid (**A**) forming 5-methylenedihydrofuran-2(3*H*)-one (**B**) and/or 2-methyl-5-oxotetrahydrofuran-2-ylpent-4-ynoate (**C**). The catalytic activity of **1**, **2** and other polynuclear Cu(I) complexes (**3–5**) was evaluated under solvent free conditions and/or solution. In the absence of solvent, catalyst **2** displays the highest activity and selectivity (75.8/23.1, **C** to **B** ratio, at 5.4% loading) while **4** reaches the highest level of A → **B** conversion (97.5 %) in solution. Selected reactions were followed by NMR and the kinetic constants calculated. A mechanism is proposed based on the equations used for the calculations. © 2014 Wiley Periodicals, Inc. J. Polym. Sci., Part A: Polym. Chem. **2014**, *52*, 3316–3323

KEYWORDS: alkynoic acid cyclization; camphor derived ligands; camphor ligands; copper; coordination polymers; Cu(I); Hartree-Fock ab initio calculations; lactones; solvent free catalysis

INTRODUCTION Copper halides are suitable scaffolds for the synthesis of Cu(I) coordination polymers with sequential copper sites assembled in a variety of structural arrangements.[1] One-dimensional Cu(I) coordination polymers with the uncommon combination of linear and tetrahedral zig–zag Cu(I) centers were obtained from camphor imine ligands[2] suggesting that camphor-type ligands have the convenient stereochemical and electronic properties to enable other wire structured Cu(I) coordination polymers. A step forward in the synthesis of camphor derived Cu(I) coordination polymers was to build copper polymers with two, rather than one CuCl strings, linked by the convenient camphor derivatives aiming at studying their properties as catalysts, a field where coordination polymers are high promising.[3–5] Cyclization processes seemed promising since Pd(II) and Pt(II) camphor complexes were found to be high active in the cyclization of alkynes or alkynols[6,7] and there is a current interest on efficient catalysts that promote the cyclization of functionalized alkynes[8–10] alkynols[11–15] or alkyne carboxylic acids[16–20] within cyclization processes that encompass purely organic[21] or metal mediated[22–24] methodologies. Catalysts developed up to now are based on expensive transition metals (Pd, Pt, Au, or Ag) and require strong basic conditions. A step forward is thus find catalysts based on cheaper metals (e.g., Cu), no added base and eventually no solvent, for the synthesis of cyclic compounds (e.g., *O*-heterocycles) with potential applications (e.g., lactones) from cyclization of alkyne carboxylic acids. Whether copper camphor coordination polymers fill the requirements above and promote the cyclization of 4-pentyn-1-oic acid was the challenge to address having the additional quiz on addition of a second substrate molecule to the *O*-heterocycle leaving pendant alkyne groups.[11,25,26]

EXPERIMENTAL

General Considerations

Synthesis of complexes and catalytic experiments were performed under nitrogen using vacuum and Schlenk techniques. The copper complexes and camphor species were prepared by published methods.[2] CuCl and CuBr were purchased from Sigma-Aldrich. The solvents were purchased from Lab-Scan, further purified by conventional techniques and distilled before use.

The IR spectra were obtained from KBr pellets using a JASCO FT/IR 4100 spectrometer. NMR spectra (^{1}H, ^{13}C, DEPT, 2D) were obtained from $CDCl_3$ or DMSO-d_6 solutions using Bruker Avance II$^+$ Spectrometer (400 MHz) and values referred to tetramethylsilane ($\delta = 0$ ppm). X-ray Photoelectron Spectra were obtained using a Kratos XSAM800. Samples were irradiated with the unmonochromatic Al Kα radiation. Experimental conditions and details about data treatment were the same as described elsewhere.[27] Sensitivity factors here used were: C 1s:0.25; O 1s:= 0.66; N 1s:0.42; Cu 2p3/2:4.2; Cl 2p:0.61. HPLC chromatograms were obtained using Jasco PU-2089 Plux Pumps interfaced with a MD-1515 Diode Array Detector. The separation was made through a YMC Pro C18 column using as eluents: H_2O (A) and CH_3CN/H_2O (B, 75/25 V/V) at the flow rate 0.7 mL/min, programmed as follows: starting (40% A, 60% B), 5 min (15% A, 85% B), 10 min (15% A, 85% B), 11 min (2% A, 98% B), 15 min (100% B), 20 min (40% A, 60% B). Chiral samples were characterized using a Dionex Ultimate 3000 equipment provided with a Lux 5u Cellulose-1 column running with a isocratic eluent program (90% hexane, 10% isopropanol with 0.9 mL/min flow).

Synthesis of Complexes

The complexes were typically obtained as amorphous compounds, on stirring copper chloride (CuCl) and the adequate camphor ligand (L) in THF (3 mL) at room temperature (RT) for about 18 h. Filtration of the precipitate, washing with *n*-pentane (ca. 6 mL), and drying under vacuum affords the Cu(I) complex.

$[(CuCl)_4\{p\text{-}C_6H_4(NC_{10}H_{14}O)_2\}]_n$ (**1**) - CuCl (0.030 g, 0.30 mmol) and 3,3′-(*p*-phenylenebis(azan-1-yl-1-ylidene))bis(1,7,7-trimethylbicyclo[2.2.1]heptan-2-one) (**e**, 0.030 g, 0.074 mmol) were stirred in THF to afford a brown precipitate. Yield 48%. ELEM. ANAL (%) for $Cu_4Cl_4C_{26}H_{32}N_2O_2$: Found: C, 38.9; N, 3.1; H, 4.0; Calc.: C, 39.2; N, 3.5; H, 3.6. IR (cm^{-1}): 1750 (υ_{CO}), 1641 (υ_{CN}), 1591 (υ_{CCarom}). ^1H NMR ($CDCl_3$, δ ppm): 7.14 (s, 4H), 2.93 (sbr, 1H), 2.17–1.70 (m, 4.0 H), 1.11 (s, 3H), 1.02 (s, 3H), 0.89 (s, 3H). ^{13}C NMR ($CDCl_3$, δ ppm): 204.9, 174.2, 145.9, 122.9, 58.2, 50.8, 45.3, 30.1, 24.4, 21.4, 17.5, 9.1.

$[(CuCl)_3(C_6H_4NC_{10}H_{14}N)]$ (**2**) - CuCl (0.108 g, 1.09 mmol) and camphorquinoxaline ($C_6H_4NC_{10}H_{14}N$, 0.10 g, 0.42 mmol) afforded the compound as an orange precipitate. Yield 78%. ELEM. ANAL for $Cu_3Cl_3C_{16}H_{18}N_2O_2 \cdot \frac{1}{2}THF$: Found: C, 38.0; N, 5.1; H, 3.5%. Calc.: C, 37.8; N, 4.9; H, 3.9. IR (cm^{-1}): 1508 (υ_{CN}). ^1H NMR (MeOH-d_4, δ ppm): 8.15–8.05 (m, 2H), 8.05–7.77 (m, 2H), 3.16 (d, $J = 4.0$, 1H), 2.20–0.90 (m, 4H), 1.48 (s, 3H), 1.18 (s, 3H), 0.64 (s, 3H). ^{13}C NMR ($CDCl_3$, δ ppm): 130.1, 129.7, 116.6, 110.4, 68.8, 32.7, 25.3, 20.5, 18.6, 10.4.

Catalytic Experiments

Solvent Free

4-pentyn-1-oic acid (**A**, 0.030 g, 0.31 mmol) was stirred under vacuum for no less than 15 min. Then nitrogen was fluxed in the Schlenk followed by addition of the copper complex. The solids were then grinded under nitrogen for 2, 6, 18, 24, or 56 h, at RT, 40 °C or 60 °C forming oily mixtures. Different loadings of catalysts were screened for reactions at 40 °C during 18 h. On completion, the reaction was stopped by addition of $CDCl_3$ and the yellow solution was immediately analyzed by NMR (^1H, ^{13}C, DEPT, 2D).

In DMSO

All solutions were prepared under nitrogen using sure seal NMR tubes. Typically, 4-pentyn-1-oic acid (**A**, 0.030 g, 0.31 mmol) was added to the catalyst (0.020 g) solution in DMSO-d_6 (ca. 0.3 mL) and the reaction was followed by NMR.

Calculations

Kinetic Constants

Data on the relative quantity of catalytic products was obtained by integration of the methylene (**B**), the methyl (**C**), or the vinyl (**D**) signals observed in the ^1H NMR spectra. The integration of the signals corresponding to the methyl groups of the camphor ligand were used as internal reference. For calculation of the constants, the unitary activity was considered as $1/100_{th}$ of the integration of the NMR signal in the spectra obtained upon 4 min reaction, normalized to the number of magnetic nuclei. A FORTRAN subroutine[7] was used to perform the numerical integration of the complete set of equations in Scheme 2 (using steps of 0.01 min). The output was then fed to a least squares routine and the generated values were optimized till convergence to experimental values was 0.992 (**2**; $T = 40$ °C), 0.999 (**2**; $T = 60$ °C) and 0.962 (**3**; global fitting of 2 loadings).

Structures

Hartree-Fock *ab initio* calculations were carried out with GAMESS-US[28] version R3 using a SBKJC basis set.[29,30] The basic repeating units (Cl-Cu-Cl, anionic and CuL, cationic) were fully optimized without any symmetry or geometric constrains and were used to generate the representative dimeric oligomer by simple translation. The oligomer was again fully optimized without symmetry or geometric restrains to obtain optimized structures for **1**, formed by sequential, linear (Cl-Cu-Cl) and tetrahedral (CuL) units [Fig. 1(above)] and **2**, formed by sequential, linear (Cl-Cu-Cl) and trigonal (L-Cu-Cl-Cu-L) units [Fig. 1(below)].

RESULTS AND DISCUSSION

Synthesis and Characterization

Camphor complexes $[\{CuCl\}_4\{p\text{-}C_6H_4(NC_{10}H_{14}O)_2\}]_n$ (**1**) and $[\{CuCl\}_3(C_6H_4NC_{10}H_{14}N)]$ (**2**) were obtained in THF, from reaction of CuCl with the camphor derivatives L1 or L2 (Fig. 2). L1 (bi-camphor) and L2 (camphorquinoxaline)[31] were chosen because they can accommodate more than one metal *per* ligand and thus bridge or chelate metal sites.

The complexes (**1** and **2**) were formulated based on NMR, FTIR, ELEM. ANAL, and further confirmed by X-ray photoelectron spectroscopy (XPS).

XPS data obtained from complexes **1** and **2**, show that the region Cu 2p displays the same shape for both complexes. As a representative example, Figure 3 depicts that region for complex **1**. A single peak (a Gaussian-Lorentzian product)

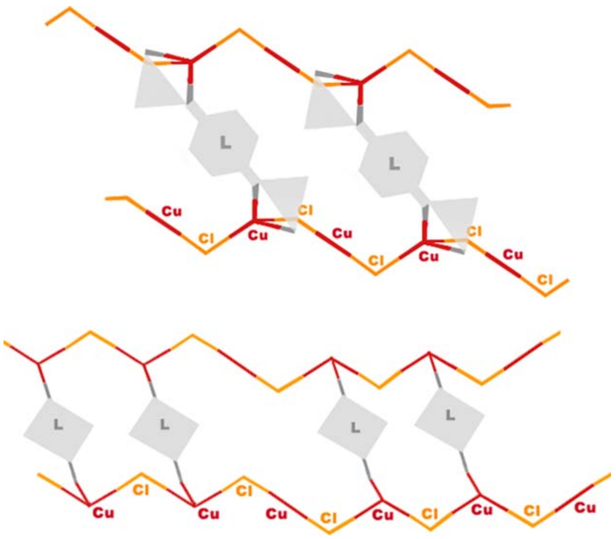

FIGURE 1 Optimized schematic structures for **1** (above) and **2** (below). [Color figure can be viewed in the online issue, which is available at wileyonlinelibrary.com.]

with a FWHM = 1.9 ± 0.1 eV, centered at 932.4 ± 0.1 eV fitted to the Cu $2p_{3/2}$ attests the oxidation state of copper as *plus* one,[2] this being further confirmed by the absence of the multiplet structure characteristic of Cu(II) in the region between the two components of the doublet (Cu $2p_{3/2}$ and Cu $2p_{1/2}$).

In what concerns the Cl 2p region data was fit with a single doublet with a spin-orbit split of 1.6 ± 0.1 eV and the Cl $2p_{3/2}$ centered at 198.5 ± 0.1 eV for complex **1** and 198.2 ± 0.1 eV for complex **2** denoting a slightly higher electronic density around chloride in complex **2** than in complex **1**. For the N 1s region, single peaks were fit centered at 400.0 ± 0.1 eV for **1** and 400.2 ± 0.1 eV for **2** which are compatible with imine nitrogen atoms bound to Cu(I).[2]

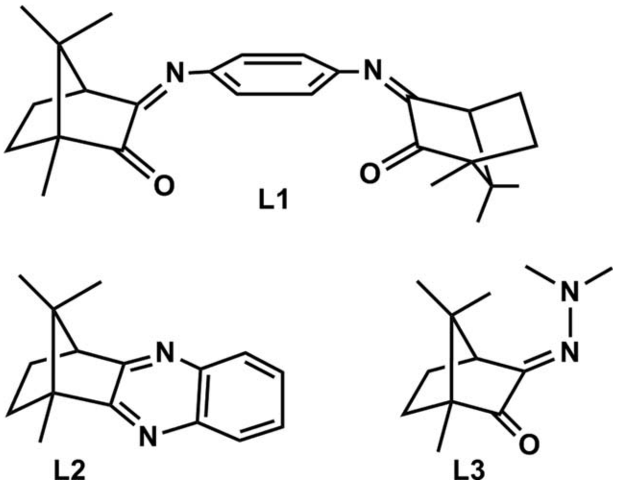

FIGURE 2 Camphor compounds used as ligands (L1 for complex **1** and L2 complex for **2**).

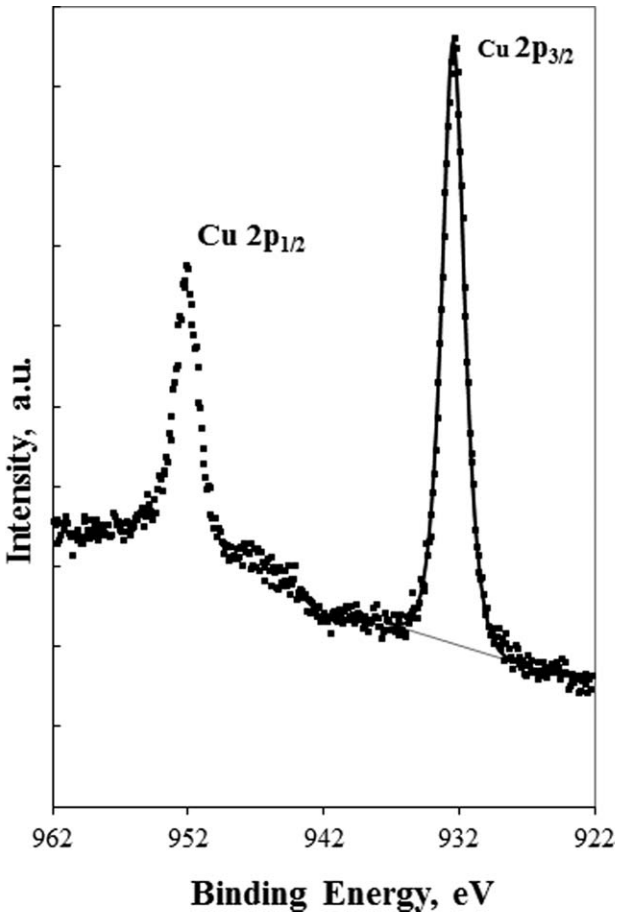

FIGURE 3 XPS data for the Cu 2p region in **1**.

The XPS quantitative analysis corroborates the expected stoichiometric ratios for complexes **1** and **2**, since the calculated values (Cu/Cl: 0.94 ± 0.1, (**1**); 0.99 ± 0.1, (**2**) and Cu/N: 2.1 ± 0.2 (1); 1.4 ± 0.1 (**2**)) closely approach the expected ones for Cu/Cl (1) and Cu/N ratios [(221 (**1**); 1.5 (**2**)].

In the absence of elucidation of the structure of complexes **1** and **2** by single-crystal X-ray diffraction, due to no suitable crystals could be obtained, XPS data fully supports the proposed formulations.

The metal to ligand ratio [3:1 (**2**), 4:1(**1**)] suggests the complexes arrange as coordination polymers such as in $[\{CuCl\}_2(Me_2NC_{10}H_{14}O)]_n$ (**3**) derived from ligand L3 (Fig. 4) that was structurally characterized.[27,32] In **3** two distinct Cu(I) units exist, one is tetrahedral and the copper atom binds to the camphor ligand (Cu-L) and the other is linear

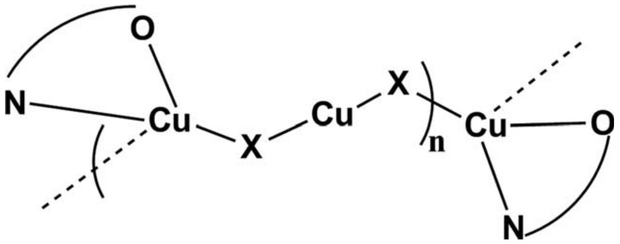

FIGURE 4 Schematic structure of $[\{CuCl\}_2(Me_2NC_{10}H_{14}O)]_n$ (**3**).

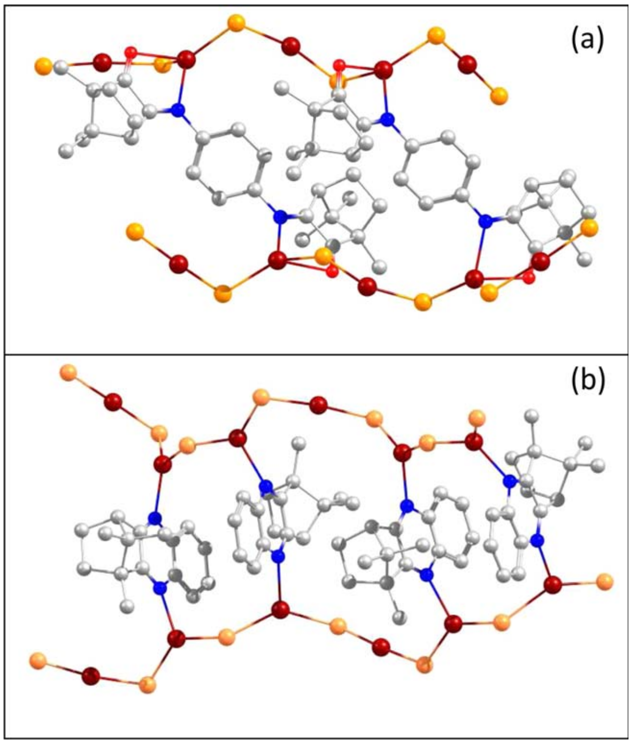

FIGURE 5 Hartree-Fock *ab initio* structure optimized for: (a) - **1**, (b) - **2**. [Color figure can be viewed in the online issue, which is available at wileyonlinelibrary.com.]

and the copper atom binds solely to the halide (Cl-Cu-Cl) (Fig. 3).

Considering that in L1 exist two N,O units of the type of that in L3 (Fig. 2), it was anticipated that two parallel Cl-Cu-Cl strings bind the ligand in $[\{CuCl\}_4\{p\text{-}C_6H_4(NC_{10}H_{14}O)_2\}]_n$ (**1**), that is, the double of the Cl-Cu-Cl units compared to $[\{CuCl\}_2(Me_2NC_{10}H_{14}O)]_n$ (**3**). Using those two building units (linear anionic, Cl-Cu-Cl and tetrahedral cationic, CuL) *ab initio* Hartree-Fock calculations were carried out to predict the geometry of the repeating unit of **1** (Fig. 5 above).

By simple translation, a dimeric oligomer was generated and fully optimized without symmetry or geometric constrains. This oligomer is representative of the structure of the coordination polymer, since extension to higher order calculations become computationally prohibitive. In the calculated structure (**1**), the bi-camphor ligand adopts a *trans* geometry in contrast with the *cis* geometry found in the free ligand.[31]

Assuming that in **2,** the N,N ligand behaves similarly to the N,O ligand in L1, *ab initio* Hartree-Fock calculations led to sequences of L-Cu-Cl-Cu-L strings linked by Cl-Cu-Cl units (Fig. 5 below) fulfilling the experimental metal to ligand ratio (3:1). The stereochemical hindrance introduced by ligand L2 precludes further coordination to the L-Cu-Cl-Cu-L units that display a trigonal arrangement. Although noncharacteristic of Cu(I) coordination number three was found in other cases.[1,33,34]

The structural parameters obtained in the optimized structures of **1** and **2** reproduce well those in compounds **3** (two polymorphs) that were structurally characterized by X-ray diffraction analysis.[2] The bond lengths calculated for the camphor ligands (e.g., C=O, 123 pm; C—N, 127 pm for **1**) are within 1 pm of the experimental ones (C=O, 123; C—N, 128 pm for **3**). The agreement is not so good in the calculated metal to camphor ligand distances (Cu-N 222 pm; Cu-O 268 pm) that are overestimated by about 20 pm compared to the corresponding values measured for **3** (202 and 247 pm). The trend is the same for the Cu-Cl bond lengths calculated (233 pm, **1**; 229 pm, **2**) and measured (211 pm, **3**) on the Cl-Cu-Cl units and those calculated (249 pm, **1**; 247 pm, **2**) and measured (227 pm, **3**) on the Cl-Cu-L units. The lack of polarization functions in the SBKJC basis set is considered to account for the observed deviation in values.

Catalytic Studies

The ability of complexes $[\{CuCl\}_4\{p\text{-}C_6H_4(NC_{10}H_{14}O)_2\}]$ (**1**) and $[(CuCl)_3(C_6H_4NC_{10}H_{14}N)]$ (**2**) as well as that of $[\{CuCl\}_2(Me_2NC_{10}H_{14}O)]_n$ (**3**), $[\{Cu(Me_2NC_{10}H_{14}O)\}_2(\mu\text{-}Cl)_2]$ (**4**), $[\{Cu(Me_2NC_{10}H_{14}O)\}_2(\mu\text{-}Br)_2]$ (**5**) for promote cyclization of 4-pentyn-1-oic acid (**A**) was evaluated. In the absence of solvent, all complexes are active catalysts for formation of lactones **B** and **C** (Scheme 1). In DMSO, the process becomes more selective and just lactone **B** forms. There is also evidence for traces of **D**.

Catalysis in the Absence of a Solvent

To establish suitable conditions for the study of the catalytic activity of complexes **1–5** on cyclization of 4-pentyn-1-oic (**A**) under solvent free conditions, complex $[\{CuCl\}_2(Me_2NNC_{10}H_{14}O)]_n$ (**3**) and **A** (solid) were grinded together for 2, 6, 18, 24, or 56 h, at RT or 40 °C. Then, the reaction (oily yellowish mixtures) was quenched by addition of $CHCl_3$ and the solution analyzed by NMR (^1H, ^{13}C). The composition of the reaction mixtures considerably varied with reaction time and temperature. Thus, for comparison of the catalytic properties of compounds **1–5** a reaction period of 18 h and a temperature of 40 °C were chosen. For completeness, the loading of catalyst was varied from 0.3 to 6.4% mol, in representative cases. Analysis of the NMR spectra of reaction mixtures showed that all complexes (**1–5**) activate the regioselectively 5-*exo-dig* cyclization of 4-pentyn-1-oic acid forming 5-

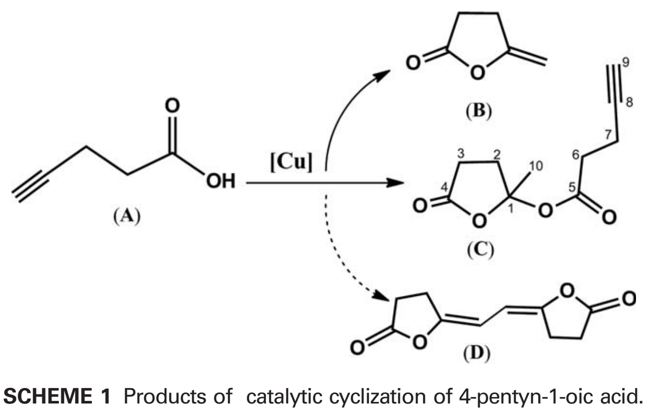

SCHEME 1 Products of catalytic cyclization of 4-pentyn-1-oic acid.

TABLE 1 Conversion of 4-pentyn-1-oic acid (**A**) into **B**, **C,** and **D** Catalyzed by Cu (I) Camphor Complexes under Solvent Free Conditions

Catalyst		Conversion (%)		
	mol %	**B**	**C**	**D**
$[\{CuCl\}_4\{p\text{-}C_6H_4(NC_{10}H_{14}O)_2\}]_n$ (**1**)	0.4	0.51	0.82	0.0
	2.4	45.4	54.6	0.0
$[(CuCl)_3(C_6H_4NC_{10}H_{14}N)]_n$ (**2**)	5.4	23.1	75.8	1.1
$[\{CuCl\}_2(Me_2NNC_{10}H_{14}O)]_n$ (**3**)	0.6	5.7	3.7	0.0
	2.6	18.6	12.3	0.0
	5.2	35.5	63.1	1.4
$[\{Cu(Me_2NNC_{10}H_{14}O)\}_2(\mu\text{-}Cl)_2]$ (**4**)	0.5	14.0	2.7	0.0
	2.5	44.2	55.3	0.5
$[\{Cu(Me_2NNC_{10}H_{14}O)\}_2(\mu\text{-}Br)_2]$ (**5**)	0.3	5.8	7.2	0.0
	1.0	23.3	28.3	0.0
	2.3	20.7	33.6	0.0
CuCl		No	products	
$CuCl_2$		No	products	

methylenedihydrofuran-2(3*H*)-one (**B**) and 2-methyl-5-oxotetrahydrofuran-2-ylpent-4-ynoate (**C**). Traces (ca. 1%) of 5,5′-(ethane-1,2-diylidene)bis(dihydrofuran-2(3H)-one (**D**) (Scheme 1) were found in reaction with **2**. Identification of compounds **B**, **C** and **C** was supported by published data (^{1}H NMR and ^{13}C NMR).[26,35,36] Compound **C** was obtained as a mixture of enantiomers that were separated by HPLC (*ee.* 65%). Formation of **C** requires cascade activation of two molecules of 4-pentyn-1-oic acid (**A**) by the Cu(I) camphor complexes. One of the molecules of **A** cyclizes, forming the *O*−heterocycle (lactone) while the other one adds to the cycle through the carboxylic acid leaving a pendant alkyne group (**C**, Scheme 1). Related processes were found in the syntheses of furan or pyran type species from alkynols catalyzed by Pt(II) or Pd(II) camphor complexes[7,11] showing that camphor complexes are prone to promote such type of processes. To exclude that the active species in the cyclization of **A** are CuCl, $CuCl_2$ (due to complexes decomposition) or the free camphor ligands, the reaction of each one of them with **A** was done separately and the mixture analyzed. No evidence for products of cyclization was found in agreement with catalysis by the polynuclear camphor copper complexes.

TABLE 2 Conversion of 4-pentyn-1-oic acid (**A**) into **B** Catalyzed by Camphor Cu (I) Complexes in DMSO[a]

Catalyst	% Catal	Temp (°C)	**B**
$[\{Cu(Me_2NNC_{10}H_{14}O)\}_2(\mu\text{-}Cl)_2]$ (**4**)	1.6	40	37.0
	1.6	60	97.5
$[\{Cu(Me_2NNC_{10}H_{14}O)\}_2(\mu\text{-}Br)_2]$ (**5**)	2.3	40	25.0
	8.1	40	42.0

[a] Snapshot made after at 52 h reaction.

The conversion of **A** into products (Scheme 1) was calculated by integration in the ^{1}H NMR spectra of the methylene (**B**), methyl (**C**), or methyne (**D**) signals, using the methyl groups of the camphor skeleton as internal reference. Data from reactions (18 h, 40 °C) shows that compounds **B**, **C,** and **D** form, the relative amounts depending on the catalyst and on its loading (Table 1). Full conversion of **A** into products requires catalysts loadings no lower than 2.5%. The process is low selective, **B** and **C** typically forming. Higher catalyst loadings favor formation of **C**. From the five polynuclear Cu(I) complexes under evaluation, complex **2** displays the highest selectivity for **C** (75.8%, Table 1) formation. Tentative increase of the catalyst loading does not improve the content in **C** due to competitive formation of **D**. The herein results show that the products distribution is controlled by the characteristics of the complex as well as the exposed surface

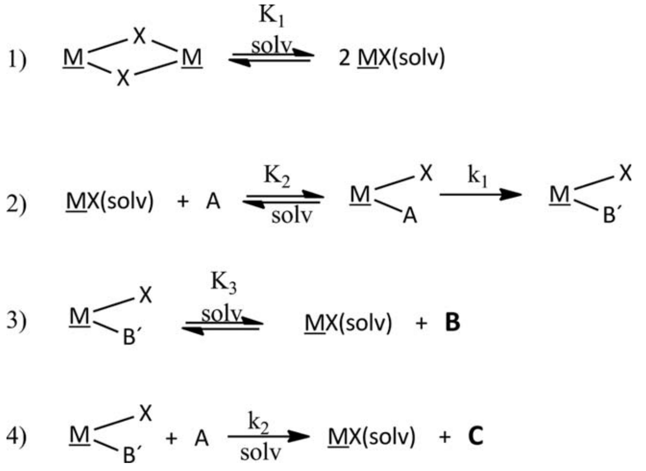

SCHEME 2 Mechanism proposed for conversion of **A** into products **B** and **C** catalyzed by complexes **2** or **3**.

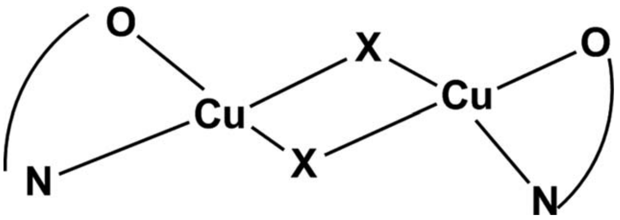

FIGURE 6 Schematic structure for **4** (X = Cl) and **5** (X = Br).

TABLE 3 Calculated Constants for Conversion of **A** into Products **B** and **C** Promoted by Catalysts **4** and **5**

Catalyst	Temp (°C)	$K_1 \times 10^5$	K_2	K_3	$k_1 \times 10^3$ (min^{-1})	$k_2 \times 10^4$ (min^{-1})
4	40	10.20	2.48	24.81	8.97	7.14
4	60	29.29	24.77	3.35	26.48	
5	40	7.13	1.09	36.48	8.39	

of catalyst, pointing to grinding efficiency as being quite relevant.

Catalysis in DMSO

The low solubility of compounds **1** and **2** in DMSO, in addition to low stability in $CHCl_3$ or MeOH for long enough periods to allow the catalytic process to reach completion, precluded the catalytic studies in solution. From the complexes under study, **4** and **5** were chosen due to their identical structures (differ just in the halide co-ligand, Fig. 6)[27] and under solvent free conditions they display quite different catalytic activities (**4** is high active, while **5** is not so, Table 1).

The reactions were followed by NMR till no **A** was detected (up to 9 days in some cases). A snapshot on the experimental data was made at 52 h reaction and the conversion into products calculated (Table 2).

Traces of **C** are detected just for periods of reaction longer than 52 h. From data (Table 2) it comes out that complex **4** performs better than complex **5** for cyclization **A**, as it did already in the absence of solvent (Table 1). Since the major difference in **4** and **5** concerns to the halide co-ligand, it is reasonable to conclude that it directs the process. In both cases the conversion increases with catalyst loading and temperature, although no full conversion is achieved in reaction with **5** after 52 hours reaction (Table 2). On the contrary, **4** promotes almost complete conversion of **A** → **B** (97.5%) at 60 °C, within a selective process that is even more efficient than cyclization of 4-pentyn-1-oic acid promoted by Au(I) catalysts.[25] The catalytic activity of **4** does not decrease appreciably upon reloading **A** for 3 times.

Kinetic Studies

To get some insight into the mechanism of cyclization of 4-pentyn-1-oic acid (**A**) catalyzed by complexes **4** and **5**, the full set of data obtained by NMR (disappearance of **A** and formation **B** and **C**) was fitted considering mechanism in Scheme 2.

Experimental and calculated data for reaction ($\mathbf{A} \rightarrow \mathbf{B} + \mathbf{C}$) catalyzed by complex **4** ($T = 40$ °C or $T = 60$ °C) is displayed in Figure 6.

Experimental and calculated data for $\mathbf{A} \rightarrow \mathbf{B}$ ($T = 40$ °C) conversion catalyzed by complex **5** at two loadings is displayed in Figure 7.

The calculated and experimental data fit to 0.992 (**2**; $T = 40$ °C), 0.999 (**2**; $T = 60$ °C), and 0.962 (**5**; global fitting for the 2.3% and 8.1% loadings) in agreement with the process in Scheme 2 that involves steps: (1) establishment of an equilibrium ($K_1 << 1$, Table 3) between the dimer complexes (**4** or **5**) and the solvated monomer {MX(solv)} (formed by break of the halide bridges and solvent coordination); (2) replacement of the solvent by **A** forming {MXA} which enables the intramolecular cyclization of **A** forming {MXB′} (kinetic control); (3) release of **B** and regeneration of {MX(solv)} within an equilibrium strongly shifted to the right

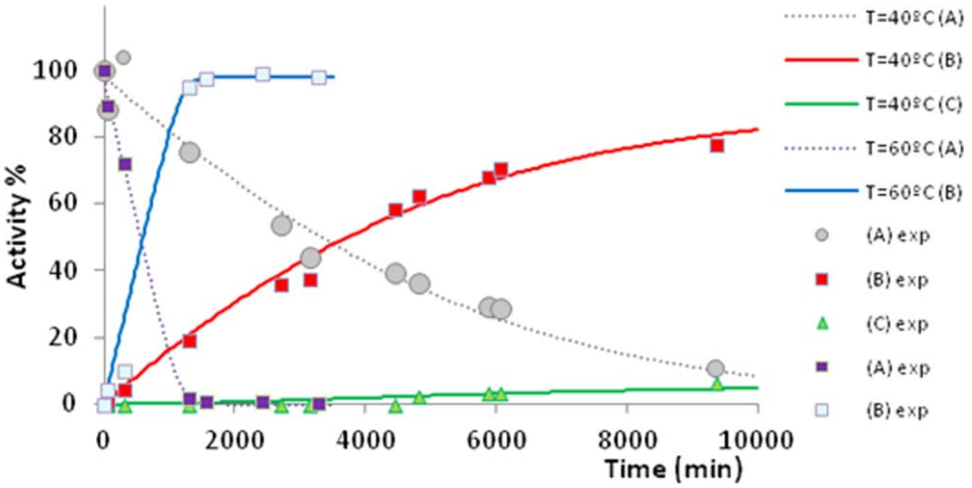

FIGURE 7 Experimental data and fittings for formation of **B** and **C** and **A** consumption catalyzed by $[\{Cu(Me_2NNC_{10}H_{14}O)\}_2(\mu\text{-}Cl)_2]$ (**4**) at 40 and 60 °C. [Color figure can be viewed in the online issue, which is available at wileyonlinelibrary.com.]

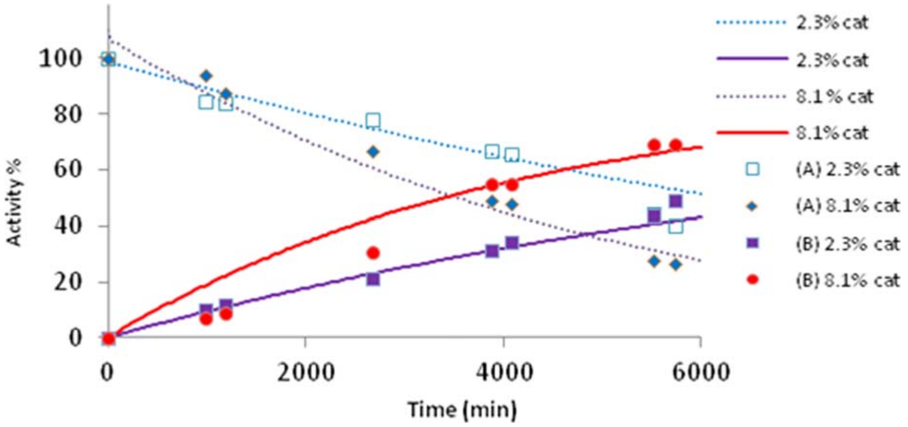

FIGURE 8 Experimental data and fittings for **A** → **B** conversion promoted by **5** at 40 °C, using catalyst loadings: 2.3% (□) or 8.1% (○). [Color figure can be viewed in the online issue, which is available at wileyonlinelibrary.com.]

($K_3 > 1$). This reactivity cycle proceeds until the concentration of **B** is high enough to shift the equilibrium (K_3) to the left, and enable formation of **C** through reaction with **A** regenerating {MX(solv)} (step 4). According to this mechanism, formation of **C** may vary from low probable ($T = 40$ °C, catalyst **4**) to impossible ($T = 60$ °C, catalyst **4**; $T = 40$ °C, catalyst **5**). At 60 °C fast consumption of **A** forming **B** (97.5%) precludes sufficient free **A** in solution, to allow formation of **C** (Fig. 7).

Considering the mechanism in Scheme 2, the constants were calculated and are displayed in Table 3.

The considerably different catalytic activities of complexes **4** and **5** are attributed to the break of the halide bridge (step 1) to generate the active species {MX(solv)} which is facile in the chloride (**4**) than in the bromide (**5**) complex (K_1, Table 3). Such trend was observed before in the polymer-dimer inter-conversion processes that are enabled in the case of the chloride complex.[27]

The cyclization process (step 2) is almost independent of the halide (k_1, Table 3) while the temperature has a great effect on it (i.e., k_1 increases by a factor of three by raising the temperature from 40 to 60 °C) as well the catalyst loading (Fig. 8).

No kinetic data could be obtained from reactions of 4-pentyn-1-oic acid with complexes **1–5** in the absence of solvent, since the experimental conditions preclude the reaction to be followed by NMR and no alternative was found. Nevertheless, from the obtained results it is reasonable to assume that the interaction of **A** with the surface of the complex promotes activation of the CC triple bond forming {**B**′} within a process controlled by the number of active sites (i.e., catalyst surface area and loading). In the absence of a solvent, diffusion is very slow and the activated species {**B**′} may remain at the surface of the catalyst enabling attack by a second **A** molecule forming **C** or may be released as **B**. Coarse or fine grinding is a parameter that can affect products distribution. As far as we know **C** has only been identified in a solvent free process catalyzed by Ag(I),[26] thus reinforcing the above proposal.

CONCLUSIONS

The set of polynuclear camphor-derived Cu(I) compounds $[(CuCl)_2L]_n$ and $[(CuL)_2(\mu\text{-}L)_2]$ was extended to the new coordination polymers $[(CuCl)_4L1]_n$ and $[(CuCl)_3L2]_n$ by using the bi-camphor (L1) or camphorquinoxaline (L2) ligands. The structures of $[(CuCl)_4L1]_n$ and $[(CuCl)_3L2]_n$ were optimized by *ab initio* Hartree-Fock calculations, showing that two side by side copper strings with sequential Cu-L; Cl-Cu-Cl (**1**) or L-Cu-Cl-Cu-L; Cl-Cu-Cl (**2**) support the ligands.

All the complexes $[(CuCl)_4\{p\text{-}C_6H_4(NC_{10}H_{14}O)_2\}]_n$ (**1**), $[(CuCl)_3(C_6H_4NC_{10}H_{14}N)]$ (**2**), $[\{CuCl\}_2(Me_2NC_{10}H_{14}O)]_n$ (**3**) and $[\{CuX(Me_2NC_{10}H_{14}O)\}_2(\mu\text{-}X)_2]$ (X = Cl, **4** or Br, **5**) are active catalysts for cyclization of 4-pentyn-1-oic acid under solvent-free conditions. Lactones 5-methylenedihydrofuran-2(3*H*)-one (**B**) and 2-methyl-5-oxotetrahydrofuran-2-ylpent-4-ynoate (**C**) were obtained as the major products. Formation of **C**, involves the *one pot* activation of two molecules of 4-pentyn-1-oic acid through a process for which compound **2** displays the higher selectivity (**C**, ca. 75%). The distribution of the products is quite different in reactions performed with or without solvent. In solution, formation of **B** versus **C** is enhanced; at 60 °C, $[\{Cu(Me_2NNC_{10}H_{14}O)\}_2(\mu\text{-}Cl)_2]$ displays the highest activity and selectivity (97.5% conversion).

Synthesis of lactones (**B**, **C**) through cyclization of 4-pentyn-1-oic acid, catalyzed by the camphor-derived Cu(I) polynuclear complexes meet the requirements for green chemistry in what concerns solvent free conditions, no need of added base and 100% atom economy.

A mechanism is proposed for cyclization of 4-pentyn-1-oic acid, based on calculation of constants by fitting the ^{1}H NMR data that highlights the relevance of the halide co-ligand (Cl or Br) in the process.

ACKNOWLEDGMENTS

The authors thank Vânia André for helpful discussions, FCT-Fundação para a Ciência e Tecnologia for financial support (Projecto Estratégico – PEst-OE/QUI/UI0100/2013), and the NMR Network for facilities.

REFERENCES AND NOTES

1 R. Peng, M. Li, D. Li, *Coord. Chem. Rev.* **2010**, *254*, 1–18.

2 T. A. Fernandes, M. F. N. N. Carvalho, A. M. Galvão, N. A. G. Bandeira, M. J. Calhorda, A. M. Botelho do Rego, *J. Polym. Sci. Part A: Polym. Chem.* **2012**, *50*, 1102–1110.

3 C. M. Doherty, D. Buso, A. J. Hill, S. Furukawa, S. Kitagawa, P. Falcaro, *Acc. Chem. Res.* **2014**, *47*, 396–405.

4 H. Furukawa, K. E. Cordova, M. O'Keeffe, O. M. Yaggi, *Science* **2013**, *341*, 499–504.

5 Y. Liu, W. Xuan, Y. Cui, *Adv. Mater.* **2010**, *22*, 4112–4135.

6 M. F. N. N. Carvalho, F. M. T. Almeida, A. M. Galvão, A. J. L. Pombeiro, *J. Organomet. Chem.* **2003**, *679*, 142–149.

7 M. F. N. N. Carvalho, A. M. Galvão, A. S. D. Ferreira, *J. Organomet. Chem.* **2009**, *694*, 2061–2068.

8 H. Rudler, P. Harris, A. Parlier, F. Cantagrel, B. Denise, M. Bellassoued, J. Vaissermann, *J. Organomet. Chem.* **2001**, *624*, 186–202.

9 C. Shu, M.-Q. Liu, Y.-Z. Sun, L.-W. Ye, *Org. Lett.* **2012**, *14*, 4958–4961.

10 N. T. Patil, A. Konala, *Eur. J. Org. Chem.* **2010**, 6831–6839.

11 M. F. N. N. Carvalho, A. S. D. Ferreira, A. M. Galvão, *Inorg. Chim. Acta* **2010**, *363*, 1767–1772.

12 J. Muzart, *Tetrahedron* **2005**, *61*, 5955–6008.

13 M. Lautens, W. Klute, W. Tam, *Chem. Rev.* **1996**, *96*, 49–92.

14 K. Tanaka, Y. Tajima, *Eur. J. Org. Chem.* **2012**, 3715–3725.

15 B. Y.-W. Man, M. Bhadhade, B. A. Messerle, *New J. Chem.* **2011**, *35*, 1730–1739.

16 S. Ito, S. Kusano, N. Morita, K. Mikami, M. Yoshifuji, *J. Organomet. Chem.* **2010**, *695*, 291–296.

17 C. Lambert, K. Utimoto, H. Nozaki, *Tetrahedron Lett.* **1984**, *25*, 5323–5326.

18 C. Xu, E. Negishi, *Tetrahedron Lett.* **1999**, *40*, 431–434.

19 W. Day, J. Katzenellenbogen, *J. Org. Chem.* **1991**, *56*, 6893–6896.

20 S. Inack-Ngi, R. Rahmani, L. Commeiras, G. Chouraqui, J. Thibonnet, A. Duchêne, M. Abarti, J.-L. Parrain, *Adv. Synth. Catal.* **2009**, *351*, 779–788.

21 B. Godoi, R. F. Schumacher, G. Zeni, *Chem. Rev.* **2011**, *111*, 2937–2980.

22 S. Y. Seo, X. Yu, T. J. Marks, *J. Am. Chem. Soc.* **2009**, *131*, 263–276.

23 I. Omae, *Appl. Organomet. Chem.* **2008**, *22*, 149–166.

24 X.-F. Wu, H. Neumann, M. Beller, *Chem. Rev.* **2013**, *113*, 1–35.

25 D. W. Lucey, J. D. Atwood, *Organometallics* **2002**, *21*, 2481–2490.

26 S. Borghèse, P. Drouhin, V. Bénéteau, B. Louis, P. Pale, *Green Chem.* **2013**, *15*, 1496–1500.

27 M. F. N. N. Carvalho, M. T. Duarte, T. A. Fernandes, A. M. Galvão, A. M. Botelho do Rego, *Inorg. Chem.* **2010**, 10330–10337.

28 M. W. Schmidt, K. K. Baldridge, J. A. Boatz, S. T. Elbert, M. S. Gordon, J. H. Jensen, S. Koseki, N. Matsunaga, K. A. Nguyen, S. Su, T. L. Windus, M. Dupuis, J. A. Montgomery, *J. Comput. Chem.* **2009**, *14*, 1347–1363.

29 W. J. Stevens, H. Basch, M. Krauss, *J. Chem. Phys.* **1984**, *81*, 6026–6033.

30 W. J. Stevens, M. Krauss, H. Basch, P. G. Jasien, *Can. J. Chem.* **1992**, *70*, 612–630.

31 T. A. Fernandes, A. M. Ferraria, A. M. Galvão, A. M. Botelho do Rego, A. C. M. Suárez, M. F. N. N. Carvalho, *J. Organomet. Chem.* **2014**. *760*, 186–196.

32 M. F. N. N. Carvalho, T. A. Fernandes, A. M. Galvão, H.-A. K. von Nidda, M. A. P. Sampaio, *Inorg. Chim. Acta* **2010**, *363*, 71–76.

33 R. D. Pike, *Organometallics* **2012**, *31*, 7647–7660.

34 A. B. Wiles, R. D. Pike, *Organometallics* **2006**, *25*, 3282–3285.

35 H. Harkat, A. Y. Dembelé, J.-M. Weibel, A. Blanc, P. Pale, *Tetrahedron* **2009**, *65*, 1871–1879.

36 H. Harkat, J.-M. Weibel, P. Pale, *Tetrahedron Lett.* **2006**. *47*, 6273–6276.